

Contribution of urbanization to warming in China

Ying Sun^{1,2}, Xuebin Zhang^{3*}, Guoyu Ren^{1,2}, Francis W. Zwiers⁴ and Ting Hu¹

China has warmed rapidly over the past half century¹ and has experienced widespread concomitant impacts on water availability, agriculture and ecosystems². Although urban areas occupy less than 1% of China's land mass, the majority of China's observing stations are situated in proximity to urban areas, and thus some of the recorded warming is undoubtedly the consequence of rapid urban development, particularly since the late 1970s^{3–5}. Here, we quantify the separate contributions of urbanization and other external forcings to the observed warming. We estimate that China's temperature increased by 1.44 °C (90% confidence interval 1.22–1.66 °C) over the period 1961–2013 and that urban warming influences account for about a third of this observed warming, 0.49 °C (0.12–0.86 °C). Anthropogenic and natural external forcings combined explain most of the rest of the observed warming, contributing 0.93 °C (0.61–1.24 °C). This is close to the warming of 1.09 °C (0.86–1.31 °C) observed in global mean land temperatures over the period 1951–2010, which, in contrast to China's recorded temperature change, is only weakly affected by urban warming influences⁶. Clearly the effects of urbanization have considerably exacerbated the warming experienced by the large majority of the Chinese population in comparison with the warming that they would have experienced as a result of external forcing alone.

The recorded warming in China since the early 1960s is almost twice as large as the global mean, and about one-third larger than the global land average temperature trend. Warming has resulted in impacts on both natural and human systems^{1,2}. There have been increased and more widespread heat waves in recent years⁷. Mountain glaciers have been in rapid retreat, resulting in changes in hydrological regimes. Permafrost has degraded, with increases in the depth and soil moisture of the active layer. Terrestrial plant species have shifted northwards. An increase in potential evaporation associated with warming has also exacerbated water deficits in arid and semi-arid regions.

Several studies have attributed the recorded warming to the combined effect of greenhouse gases and other anthropogenic influences^{7–11}. One study also links the warming to large-scale climate variability, including variability in tropical Indian Ocean sea surface temperature¹², which may itself be a response to anthropogenic forcing. In addition, many studies have pointed to rapid urbanization since the late 1970s as an important factor^{4,13–16}, especially at local scales, where these development influences may have contributed more than 40% of the observed warming in some cases^{13,15}.

Overestimation of the warming of the Chinese landmass owing to the proximity of the majority of observing stations to developing urban areas complicates the quantification of warming to different causes and the assessment of the resulting impacts. The widespread impacts described above are associated with less warming overall

than recorded in the urban-region-dominated observing system. Previous estimates of the urbanization effect rely heavily on differences in urban and rural temperature trends. However, there are increasingly fewer stations in China that are completely free of urban influences^{5,17}, probably resulting in underestimation of the urban warming influence. On the other hand, urban centres house more than half of the Chinese population^{3,5}, which means that for the majority of Chinese citizens, urban warming further increases the impacts of climate change that they experience, and requires additional adaptation measures. For example, the average daily minimum temperature in the central urban area of Beijing was 2.9 °C higher than in the suburbs during the 2–6 July 2010 heat-wave episode¹⁸.

The urbanization effect has not generally been considered in formal detection and attribution analyses because its contribution to observed warming is small on global scales⁶ and because of difficulties in removing it from observational data. Furthermore, previous studies^{7–11} have not quantified the effects of individual groups of large-scale external forcing agents on China. Here we quantify the separate contributions of multiple important external forcing factors—including urbanization (URB), greenhouse gases (GHGs), other anthropogenic forcing (OANT, predominately aerosols), and natural forcing (NAT, solar and volcanic combined)—to the warming recorded in China's temperature records, using an optimal fingerprinting technique^{19–21}.

We use monthly mean temperatures from more than 2400 observing stations (Supplementary Fig. 1) for the period 1961–2013, when the monitoring network became sufficiently dense and reliable (Supplementary Fig. 2). The station data were homogenized using the method described in ref. 22.

The pattern of urbanization-induced warming (URB) that is specified in our optimal fingerprinting analysis is based on observed urban–rural station differences. Rural stations are identified using a procedure that accounts for station history, population, the size of the built-up area and other factors (ref. 5, Supplementary Fig. 1 for the distribution of stations). Temperature differences between stations classified as urban and rural are used to estimate the spatiotemporal pattern of urbanization-induced warming (see Supplementary Information for details). This pattern shows differences between Eastern and Western China that coincide with differences in the rate and extent of urban development²³, with Eastern China experiencing earlier and stronger warming than Western China, and that plateaus sooner than Western China (Fig. 1). This is an expected effect as urban heat islands expand to include increasing numbers of station locations^{4,17,24}. The red lines in Fig. 1 indicate the urban warming signal pattern (URB) used in the optimal fingerprinting analysis. The area-weighted average of the signal patterns for Eastern and Western China has a linear trend of approximately 0.27 °C over the period 1961–2013, consistent with previous estimates of urbanization-induced warming in the Chinese

¹National Climate Center, Laboratory for Climate Studies, China Meteorological Administration, Beijing 100081, China. ²Joint Center for Global Change Studies, Beijing 100875, China. ³Climate Research Division, Environment and Climate Change Canada, Toronto, Ontario M3H 5T4, Canada. ⁴Pacific Climate Impacts Consortium, University of Victoria, Victoria, British Columbia V8W 2Y2, Canada. *e-mail: Xuebin.Zhang@Canada.ca

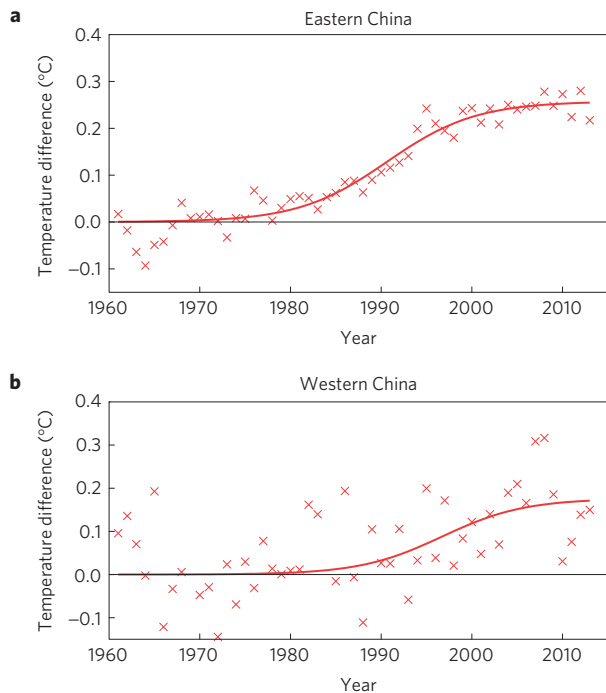


Figure 1 | Estimate of urbanization effects on temperature change.

a,b, Differences (red crosses) between regionally averaged annual mean temperatures for urban and rural stations for Eastern China (**a**) and Western China (**b**). The red lines show the logistic curves fitted to the data that represent the urbanization effect signal patterns used in the detection and attribution analyses (see Supplementary Information for details).

temperature record^{14–16,25}. However, as it is difficult to fully segregate rural and non-rural stations, we have more confidence in the URB warming pattern than in this direct estimate of the magnitude of the URB effect. We therefore use optimal fingerprinting analysis to adjust the estimated magnitude.

Adjustments to the magnitude of the URB signal must be made in the context of other factors that have also influenced China's temperatures²⁶. The spatiotemporal patterns of temperature change that are expected from the large-scale external forcings are estimated from simulations by global climate models participating in the Coupled Model Intercomparison Project phase 5 (CMIP5, ref. 27) using different combinations of external forcings (Supplementary Information).

China's recorded annual mean temperatures increased by 1.44 °C over the period 1961–2013. The observed warming is consistent with the range of multi-model-simulated climate responses to ALL forcing, but is inconsistent with the simulated responses to NAT forcing (Fig. 2). Contrary to global mean temperature²⁸, the warming in the multi-model mean response to ALL forcing for China is smaller than observed. The model response to NAT forcing is dominated by the episodic influence of large volcanic eruptions, which is clearly seen in both the NAT and ALL simulations, and corresponds well with observed changes (Fig. 2).

The fingerprint method scales the expected climate response patterns to best fit the observations. Figure 3 shows the scaling factors and their 90% confidence intervals for annual mean temperature when the observed temperature is regressed simultaneously onto two signals (including ALL and URB) and four signals (including GHG, OANT, NAT and URB), respectively. It should be noted that the approach to constructing the URB fingerprint, using an empirical approach constrained by observations and physical reasoning, is structurally different from the construction of the other fingerprints, which use an end-to-end approach in which physical

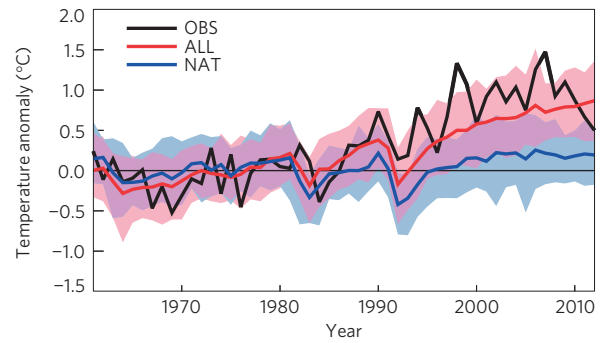


Figure 2 | Observed and simulated mean temperature change in China.

Annual mean temperature anomalies relative to the 1961–1990 average. Black, red and blue lines show observations and multi-model responses to ALL and NAT forcings, respectively. The shading indicates the 5–95% ranges of the ALL (pink) and NAT (light blue) responses in individual simulations, with the overlap in the range shown as dark mauve. The ALL forcing responses for 2006–2012 are extended using RCP4.5 simulations. Supplementary Table 1 lists the climate models and number of simulations used in the study.

principles as embodied in climate models are used to directly estimate climate response from forcing. A caveat, therefore, is that URB fingerprint uncertainty is not as well understood as that of the other fingerprints. In both cases, a residual consistency test²¹ indicates a good fit of the regression models. ALL and URB are both detected in the two-signal analysis and have scaling factor estimates consistent with the value one, indicating that their influences on the observations can be separated from each other. The best estimate of the ALL scaling factor is less than 1, suggesting a possible overestimation of the ALL response by the models. The best estimate of the URB scaling factor is larger than 1 at 1.8, suggesting that the observed temperature difference between urban and rural stations substantially underestimates the urbanization effect, consistent with an increasing urbanization influence on nominally rural stations, and previous suggestions that the current estimates of urbanization effects may be conservative owing to the difficulties in identifying rural stations that are free of urban influences¹³. Results are similar when the individual components of the external forcing (GHG, OANT and NAT) are included in the regression analysis. The scaling factors for GHG, OANT, NAT and URB are all greater than zero, and consistent with one, indicating that the influence of these individual factors can be separately identified in the observed temperature changes. The estimated URB scaling factor is again larger than one, providing a consistent assessment that the estimated URB signal may have underestimated the magnitude of the urbanization effect. This identification of URB signal in both the two-signal and the four-signal analyses is also robust against sampling uncertainty in the URB signal pattern (see Supplementary Information), which increases our confidence in the detection results.

We further estimated the warming attributable to the urbanization effect, ALL forcing, and the OANT, GHG and NAT components of ALL forcing, by computing trends in the ALL, OANT, GHG and URB signals and then multiplying them by the respective estimates of scaling factors (Fig. 4). The linear trend in the observed annual mean temperature is 1.44 °C (90% confidence interval 1.22–1.66 °C), of which 0.93 °C (0.61–1.24 °C) and 0.49 °C (0.12–0.86 °C) can be attributed to ALL and URB, respectively. The warming in China's temperature record that is attributable to urbanization is substantially larger than that for the global land surface average, which is unlikely to be more than 10% of the measured trend over the twentieth century⁶, and substantially larger than the estimate obtained by comparing nominally rural stations with non-rural stations. Both the magnitude and time

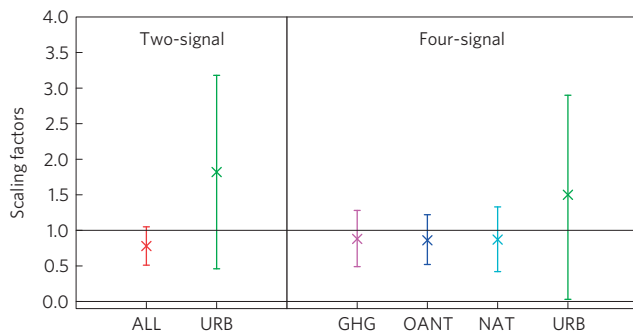


Figure 3 | Scaling factors for temperature change. Best estimates of the scaling factors that scale ALL and URB signal patterns in the two-signal analysis and URB, GHG, OANT and NAT signal patterns in the four-signal analysis to match the observed temperature anomalies and their 5–95% uncertainty ranges for annual mean temperature.

evolution of urban warming we estimated are, however, consistent with a previous observational estimate⁴ obtained by comparing changes in Chinese land area temperature with changes in adjacent sea surface temperatures. Of the three individual components of ALL, we estimate that GHG would have warmed China by 1.24 °C (0.75–1.76 °C) if it had acted on its own. The best estimate of the offsetting cooling due to OANT, which is dominated by aerosols²⁹, is 0.43 °C (0.24–0.63 °C). That is, about 35% of GHG-induced warming is offset by the OANT cooling effect, which is in-line with the estimate for global mean temperature³⁰ for 1951–2010. The influence of NAT on temperature, which is mainly due to volcanic activity, is detectable. NAT forcing may have also contributed a small warming of 0.21 °C (0.10–0.31 °C), due mostly to reduced volcanic activity towards the end of the time period, although CMIP5 simulations may not have fully accounted for the cooling effect of volcanic forcing over the most recent 15 years³¹.

To assess the robustness of the above findings, we repeated the calculation on the basis of five-year-mean series rather than three-year-mean series (see Methods). Results for the ALL and URB effects in the two-signal analysis are essentially the same as for the analysis of the three-year-mean series, although scaling factors differ slightly. In the four-signal analysis, the influence of OANT and URB are not separately detected. We also conducted two-signal and four-signal analyses for Eastern and Western China. The results are less robust, which is consistent with increased difficulty in detection and attribution for smaller regions and sub-annual averages owing to the lower signal-to-noise ratios, because less natural internal variability is filtered out when averaging over smaller areas and periods, and because there is more uncertainty in signal estimates, including the URB signal.

Multiple external factors have clearly contributed to the warming that is evident in China's temperature records. The most important factor is undoubtedly the increase in atmospheric greenhouse gases, resulting in warming comparable to the observed temperature trend. About a third of this warming is offset by the cooling effect of other anthropogenic forcing agents (OANT), which is dominated by aerosols at the global scale²⁹. Natural forcing may have also resulted in a small warming. Urbanization is the second most important contributor, accounting for about a third of the observed warming in China, and essentially eliminating the offsetting effect of OANT. This is substantially larger than the assessed impact of urbanization on global land area mean surface air temperatures⁶. The warming that China has experienced becomes consistent with that seen in the global land area mean surface air temperatures when considering only the influence of the large-scale forcing factors. Clearly, urbanization has exacerbated anthropogenically induced warming for urban populations in China.

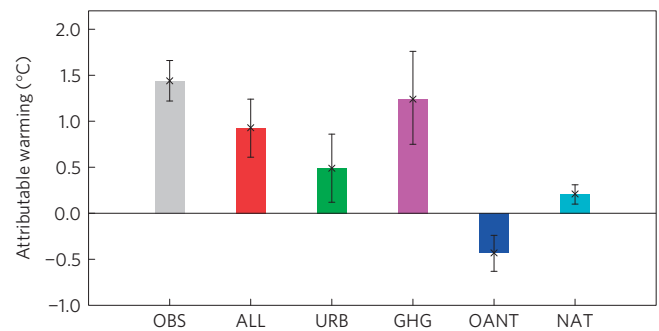


Figure 4 | Attributable warming from different contributors. Best estimate of the observed annual mean temperature trends and attributable warming due to ALL and URB from the two-signal analysis, and due to GHG, OANT and NAT from the four-signal analysis, along with their 5–95% uncertainty range.

The contamination of temperature records by rapid urbanization effects may be a more widespread problem than has been reported; it may influence recorded regional warming in other parts of the developing world, where very rapid urban development is also taking place. Our approach offers a means to more completely characterize the urbanization influence in regional temperature records that can be replicated elsewhere. This is important not only for the understanding the causes of past climate change; it also has large implications for climate change adaptation. Urban populations represent 54% of the world population, and are projected to continue to grow, with faster rates in Africa and Asia, to 66% by 2050³². As the urban heat-island effect cannot be easily reversed once established, urban populations will be impacted by the combined effect of greenhouse gas- and urbanization-induced warming. Adaptation measures appropriate to urban environments, such as green roofs, urban forests and passive cooling of buildings³³, may provide a cost-effective means for limiting the additional impacts of the urban warming influence.

Methods

Methods and any associated references are available in the [online version of the paper](#).

Received 26 June 2015; accepted 20 January 2016; published online 14 March 2016

References

- Committee of Chinese National Assessment Report on Climate Change *Third China's National Assessment Report on Climate Change* (in Chinese) (China Science Press, 2016).
- Qin, D. H., Ding, Y. J. & Mu, M. (eds) *Climate and Environment Changes in China (Synthesis Report)* 87 (in Chinese) (China Meteorological Press, 2012).
- United Nations Development Program *China Human Development Report 2013. Sustainable and Liveable Cities: Toward Ecological Urbanisation* 103 (China Translation and Publishing Corporation, 2013).
- Jones, P. D., Lister, D. H. & Li, Q. Urbanization effects in large-scale temperature records, with an emphasis on China. *J. Geophys. Res.* **113**, D16122 (2008).
- Ren, G. *et al.* An integrated procedure to determine reference station network for evaluating and adjusting urbanization bias in surface air temperature data. *J. Appl. Meteorol. Climatol.* **54**, 1248–1266 (2015).
- Hartmann, D. L. *et al.* in *IPCC Climate Change 2013: The Physical Science Basis* (eds Stocker, T. F. *et al.*) 187–194 (Cambridge Univ. Press, 2013).
- Sun, Y. *et al.* Rapid increase in the risk of extreme summer heat in Eastern China. *Nature Clim. Change* **4**, 1082–1085 (2014).
- Ding, Y. H. *et al.* National assessment report on climate change (I): climate change in China and its future trend. *Adv. Clim. Change Res.* **2**, 3–8 (2006).

9. Zhang, X., Zwiers, F. W. & Stott, P. A. Multimodel multisignal climate change detection at regional scale. *J. Clim.* **19**, 4294–4307 (2006).
10. Wen, H. Q., Zhang, X., Xu, Y. & Wang, B. Detecting human influence on extreme temperatures in China. *Geophys. Res. Lett.* **40**, 1171–1176 (2013).
11. Xu, Y., Gao, X. J., Shi, Y. & Zhou, B. T. Detection and attribution analysis of annual mean temperature change in China. *Clim. Res.* **63**, 61–71 (2015).
12. Zhao, P. *et al.* Trend of surface air temperature in eastern China and associated large-scale climate variability over the last 100 years. *J. Clim.* **27**, 4693–4703 (2014).
13. Ren, G. Y., Zhou, Y. Q. & Chu, Z. Urbanization effect on observed surface air temperature trend in North China. *J. Clim.* **21**, 1333–1348 (2008).
14. Ren, G. Y. & Zhou, Y. Q. Urbanization effects on trends of extreme temperature indices of national stations over mainland China, 1961–2008. *J. Clim.* **27**, 2340–2360 (2014).
15. Yang, X., Hou, Y. & Chen, B. Observed surface warming induced by urbanization in east China. *J. Geophys. Res.* **116**, D14113 (2011).
16. Zhang, A. Y. *et al.* Urbanization effect on surface air temperature trends over China. *Acta Meteorol. Sin.* **68**, 957–966 (2010).
17. Wang, F., Ge, Q., Wang, S., Li, Q. & Jones, P. D. A new estimation of urbanization's contribution to the warming trend in China. *J. Clim.* **28**, 8923–8938 (2015).
18. Zhang, L., Ren, G. & Ren, Y. Identification of urban heat island (UHI) effect in a single extreme high temperature event. *Clim. Environ. Res.* **20**, 167–176 (2015).
19. Hegerl, G. C. *et al.* Multi-fingerprint detection and attribution of greenhouse-gas and aerosol-forced climate change. *Clim. Dynam.* **13**, 613–634 (1997).
20. Allen, M. R. & Stott, P. A. Estimating signal amplitudes in optimal fingerprinting. Part I: Theory. *Clim. Dynam.* **21**, 477–491 (2003).
21. Ribes, A., Planton, S. & Terry, L. Application of regularised optimal fingerprinting to attribution. Part I: method, properties and idealised analysis. *Clim. Dynam.* **41**, 2817–2836 (2013).
22. Xu, W. H. *et al.* Homogenization of Chinese daily surface air temperatures and analysis of trends in the extreme temperature indices. *J. Geophys. Res.* **118**, 9708–9720 (2013).
23. Tan, M. *et al.* Urban population densities and their policy implications in China. *Habitat Int.* **32**, 471–484 (2008).
24. Jones, P. D. & Lister, D. H. The urban heat island in Central London and urban-related warming trends in Central London since 1900. *Weather* **64**, 323–327 (2009).
25. Wang, F. & Ge, Q. S. Estimation of urbanization bias in observed surface temperature change in China from 1980 to 2009 using satellite land-use data. *Chin. Sci. Bull.* **57**, 1708–1715 (2012).
26. Hegerl, G. C. *et al.* in *Meeting Report of the Intergovernmental Panel on Climate Change Expert Meeting on Detection and Attribution of Anthropogenic Climate Change* (eds Stocker, T. F. *et al.*) 1–8 (IPCC Working Group I Technical Support Unit, University of Bern, 2010).
27. Taylor, K. E., Stouffer, R. J. & Meehl, G. A. An overview of CMIP5 and the experiment design. *Bull. Am. Meteorol. Soc.* **93**, 485–498 (2012).
28. Fyfe, J. C., Gillett, N. P. & Zwiers, F. W. Overestimated global warming over the past 20 years. *Nature Clim. Change* **3**, 767–769 (2013).
29. Bindoff, N. L. *et al.* in *IPCC Climate Change 2013: The Physical Science Basis* (eds Stocker, T. F. *et al.*) 867–931 (Cambridge Univ. Press, 2013).
30. Jones, G. S., Stott, P. A. & Christidis, N. Attribution of observed historical near surface temperature variations to anthropogenic and natural causes using CMIP5 simulations. *J. Geophys. Res.* **118**, 4001–4024 (2013).
31. Santer, B. *et al.* Volcanic contribution to decadal changes in tropospheric temperature. *Nature Geosci.* **7**, 185–189 (2014).
32. Revi, A. *et al.* in *IPCC Climate Change 2014: Impacts, Adaptation, and Vulnerability* (eds Field, C. B. *et al.*) 535–612 (Cambridge Univ. Press, 2014).
33. *World Urbanization Prospects: The 2014 Revision, Highlights* (ST/ESA/SER.A/352) 32 (United Nations, Department of Economic and Social Affairs, Population Division, 2014).

Acknowledgements

We thank G. Flato, A. Cannon and K. Anderson for their comments. Y.S., T.H. and G.R. are supported by China funding agencies through multiple grants: 2012CB955900, GYHY201406020, 2012CB417205, GYHY201206012. We acknowledge the Program for Climate Model Diagnosis and Intercomparison and the World Climate Research Programme's Working Group on Coupled Modelling for their roles in making the WCRP CMIP multi-model data sets available.

Author contributions

X.Z., Y.S. and F.W.Z. designed the analysis. Y.S., X.Z. and T.H. conducted the analysis. Y.S., X.Z. and F.W.Z. wrote the paper. G.R. identified the rural stations for the estimation of the urbanization effect in temperature and helped in the analysis and the interpretation of the urbanization effect.

Additional information

Supplementary information is available in the [online version of the paper](#). Reprints and permissions information is available online at www.nature.com/reprints. Correspondence and requests for materials should be addressed to X.Z.

Competing financial interests

The authors declare no competing financial interests.

Methods

We use a total least squares optimal fingerprinting approach^{19,20} for detection and attribution, which uses a generalized linear regression model to represent observed changes as a linear combination of signals. To assess the relative contributions of external forcing and the regional urbanization effect to the observed temperature changes, we first regress the observed temperatures onto the patterns of climate responses to all external historical forcings combined (ALL) and our estimate of the urbanization effect (URB) in a two-signal setting such that

$$T_{\text{OBS}} = \beta_{\text{ALL}}(T_{\text{ALL}} - \nu_{\text{ALL}}) + \beta_{\text{URB}}(T_{\text{URB}} - \nu_{\text{URB}}) + \epsilon$$

where T_{OBS} is a vector of observed temperature anomalies, T_{ALL} and T_{URB} are signal patterns for ALL and URB, ν_{ALL} and ν_{URB} are noise from internal variability in the ALL and URB signal patterns, β_{ALL} and β_{URB} are scaling factors and ϵ is the regression residual.

We then quantify contributions to temperature change from individual factors by simultaneously regressing the observed temperature changes onto the GHG, OANT, NAT and URB signal patterns in a four-signal setting such that

$$T_{\text{OBS}} = \beta_{\text{GHG}}(T_{\text{GHG}} - \nu_{\text{GHG}}) + \beta_{\text{OANT}}(T_{\text{OANT}} - \nu_{\text{OANT}}) \\ + \beta_{\text{NAT}}(T_{\text{NAT}} - \nu_{\text{NAT}}) + \beta_{\text{URB}}(T_{\text{URB}} - \nu_{\text{URB}}) + \epsilon$$

where T_{GHG} , T_{OANT} and T_{NAT} are signal patterns for GHG, OANT and NAT, ν_{GHG} , ν_{OANT} and ν_{NAT} are noise in the corresponding signal patterns, and β_{GHG} , β_{OANT} and β_{NAT} are the corresponding scaling factors. The URB scaling factor obtained in the two-signal analysis might be different from that obtained in the four-signal analysis. If this is the case, we use the scaling factor from the two-signal analysis when computing warming attributable to URB, as scaling factors estimated from the latter should in general have smaller uncertainty.

The observational vector, T_{OBS} , which describes the spacetime evolution of temperatures, is comprised of non-overlapping three-year-mean temperatures over

two spatial dimensions representing Eastern and Western China. The use of three-year averages is a compromise between suppressing natural variability, particularly at inter-annual timescales, and the desire to be able to detect the effects of natural forcing, including the relatively short-lived responses to volcanic activity. The 52-year record (1961–2012) produces 17 non-overlapping three-year averages plus one additional year, providing 18 values. The east–west partitioning divides the country into two regions, such that the eastern domain has a much higher concentration of urban development than the western domain²³. This produces a 36-dimensional observational vector that accommodates a spatial contrast in the URB pattern to help distinguish the urban warming signal from other signals. Climate model segments from forced and control simulations are processed identically into 36-dimensional vectors.

The scaling factors are estimated using the total least squares method^{19,20} so as to account for sampling uncertainties in the signal patterns. For the model-simulated signals, sampling uncertainty is inversely proportional to the number of model runs, or equivalent model runs when addition or subtraction of signals is used. The sampling uncertainty of the URB pattern is different from that of model-simulated signals. In this case, we effectively use the ordinary least squares approach to estimate the URB signal scaling factor by specifying very low URB signal sampling uncertainty (0.01% of model-simulated internal variability). We then assess the robustness of the detection results using a bootstrapping procedure that accounts for URB signal sampling uncertainty (see Supplementary Information).

A given signal is detected in the observations if the corresponding scaling factor is significantly greater than zero. If the signal is detected, we go on to determine whether the estimated scaling factor is consistent with one, which is information that helps establish confidence in quantifying the contribution of that signal to the observed change (that is, attribution). The goodness of fit of the regression is further evaluated with a residual consistency test, which determines whether the magnitude of the estimated residuals ϵ is consistent with internal variability as simulated by unforced climate models. Further details on the data and methods are given in the Supplementary Information.